HHS Public Access

Author manuscript

Chemistry. Author manuscript; available in PMC 2017 October 27.

Published in final edited form as:

Chemistry. 2017 August 10; 23(45): 10744–10748. doi:10.1002/chem.201702302.

Selectivity of C–H *vs.* C–F Bond Oxygenation by Homo- and Heterometallic Fe_4, Fe_3Mn, and Mn_4 Clusters

Dr. Graham de Ruiter[a], **Kurtis M. Carsch**[a], **Dr. Michael K. Takase**[a], and **Prof. Theodor Agapie**[a]

[a]Department of Chemistry and Chemical Engineering, California Institute of Technology; MC 127-72, Pasadena, California 91125, (USA)

Abstract

A series of tetranuclear $[LM_3(HFArPz)_3OM']$[OTf]$_2$ (M, M′ = Fe or Mn) clusters that displays 3-(2-fluorophenyl)pyrazolate (HFArPz) as bridging ligand is reported. With these complexes manganese is demonstrated to facilitate C(sp^2) –F bond oxygenation via a putative terminal metal-oxo species. Moreover, the presence of both *ortho* C(sp^2) –H and C(sp^2) –F bonds in proximity provides an opportunity to investigate the selectivity of intramolecular C(sp^2) –X bond oxygenation (X = H or F) in these isostructural compounds. With iron as the apical metal center (M′ = Fe) C(sp^2) –F bond oxygenation occurs almost exclusively, whereas with manganese (M′ = Mn) the opposite reactivity is preferred.

Graphical Abstract

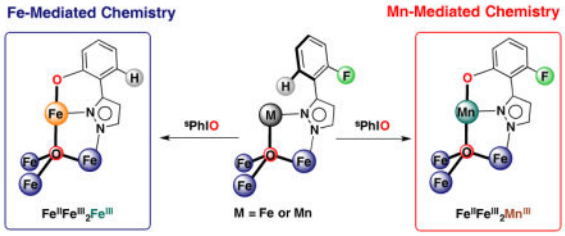

The selectivity of intramolecular C(sp^2)–H vs. C(sp^2)–F bond oxygenation is examined with a new series of $[LM_3(PhPz)_3OM']$[OTf]$_2$ (M = M′ = Fe or Mn) clusters. The distribution of metal centers within these clusters provide insight into how a single metal center (**Fe** vs. **Mn**) can control the selectivity in observed oxygenation chemistry. While for iron (M′ = Fe) essentially exclusive C(sp^2)–F bond oxygenation was observed, with manganese (M′ =Mn), C(sp^2)–H oxygenation is preferred.

Keywords

C–H and C–F bond oxygenation; multimetallic complexes; oxygen atom transfer; dehalogenation; clusters

Correspondence to: Theodor Agapie.

Terminal high-valent metal oxo species play important roles in many biological relevant transformations,[1] including the oxidative metabolism of xenobiotics.[2] An important step in the metabolism of these compounds, which includes polyaromatic hydrocarbons (PAHs) and pharmaceuticals, is aromatic C(sp^2)–H bond hydroxylation.[3] Replacing these aromatic C(sp^2)–H bonds with fluorine increases metabolic stability,[4] and is an approach regularly employed by the pharmaceutical industry to improve the bioavailability of drugs.[5] The prevalence of fluorine containing drugs raises important questions regarding the mechanism and regioselectivity of fluoroarene hydroxylation by terminal high-valent metal oxo moieties.

In vivo/vitro studies with cytochrome P450's have shown that C(sp^2)–H bond hydroxylation is the preferred reactivity pathway in various substituted fluorobenzenes.[6] Aromatic C(sp^2)–F bond hydroxylation, in contrast, is only observed in hexafluorobenzene[7] or in *para*-substituted fluoro anilines[8] and phenols.[9] Other substitution patterns (i.e. *meta* or *ortho*) result in significant C(sp^2)–H hydroxylation.[8a] These studies thus demonstrate a clear preferences for C(sp^2)–H hydroxylation of fluorinated benzenes by cytochrome P450.

Fewer studies have been reported on the selectivity of fluoroarenes oxygenation with synthetic reagents. While C(sp^2)–H bond hydroxylation of aromatic substrates by high-valent metal-oxo species is known,[10] aromatic C(sp^2)–F bond hydroxylation is exceedingly rare.[11] Only in a few instances the direct involvement of terminal high-valent metal-oxo species has been demonstrated.[11d, 11e] Cases that display chemoselective C(sp^2)–F hydroxylation of fluorobenzenes by metal-oxo species are even rarer.[12] Exclusive C(sp^2)–F bond hydroxylation *ortho* to a phenoxide moiety was observed with a dioxo-bridged copper complex.[12b] Selective hydroxylation of 4-fluorophenol was reported with a P450 mimic.[12c] However, no C–F bond activation was observed upon removing the hydroxyl substituent (e.g. in 4-fluorotoluene),[12c] suggesting that C(sp^2)–H bond hydroxylation remains the preferred reactivity pathway with a synthetic terminal high-valent metal oxo species. A more extensive study was reported with a N-bridged diiron phthalocyanine complex that selectively defluorinates arenes in the presence of other C–H bonds.[12a] Systematic studies of the structural features of metal complexes that affect the selectivity of C–H *vs.* C–F bond oxygenation are therefore very rare. Herein, we report a new series of iso-structural metal complexes $[LM_3(HFArPz)_3OM']$[OTf]$_2$ (Scheme 1: **1**, M = M′ = Fe; **2**, M = Fe, M′ = Mn; **3**, M = M′ = Mn) that exhibit opposite selectivity in the intramolecular oxygenation of 3-(2-fluorophenyl)pyrazolate (HFArPz) as a function of the identity of the metal M.

Recently we reported the intramolecular C–H and C–F bond oxygenation by multimetallic complexes of the type $[LM_3(X_2ArPz)_3OM]$[OTf]$_2$ (M = Fe or Mn; X = H or F).[11b, 11c] The observed reactivity most likely resulted from putative Fe^{IV}- and Mn^{IV}-oxo moieties, generated from iodosobenzene adducts.[13] In those cases, only one type of bond is sterically accessible for activation, therefore exclusive C–H or C–F oxygenation is observed. Given the scarcity of information about the metal complex motifs that govern the selectivity of C(sp^2)–H vs. C(sp^2)–F bond oxygenation we used a multinuclear platform to investigate the selectivity for series of structurally related complexes. Using our previously reported synthetic methodology,[11c] we synthesized $[LFe_3(HFArPz)_3OFe]$[OTf]$_2$ (**1**). The crystal

structure of **1** (Figure S25) shows the apical iron (Fe4) center coordinated by a μ_4-oxo moiety and three 3-(2-fluorophenyl)pyrazalote donors. The aryl groups display both *ortho* C(sp^2)–H and C(sp^2)–F bonds. Based on charge balance, and on the Fe1–O1 (1.915(3) Å), Fe2–O1 (1.938(3) Å), and Fe3–O1 (2.144(3) Å) bond distances, the iron oxidation states in **1** are assigned as $[LFe^{III}_2Fe^{II}(HFArPz)_3OFe^{II}][OTf]_2$, and are in agreement with those observed in previously reported complexes.[11c, 14]

With complex **1** in hand, the selectivity in C(sp^2)–H vs. C(sp^2)–F bond oxygenation was investigated. Treating **1** with 2-(*tert*-butylsulfonyl)-iodosobenzene (^{s}PhIO; 2.0 equiv.) resulted in rapid intramolecular oxygenation as judged by electrospray ionization mass spectrometry (Figure 1C). Analysis of an aliquot of the reaction mixture shows that three major species are present. No free ligand (*m/z* = 859.0) or other known multinuclear complexes was observed by mass spectrometry. The major peak at *m/z* = 787.59 is consistent with $[LFe_3(HFArPz)_2(OArPz)OFe][OTf]_2$ (**4**), suggesting C(sp^2)–F bond oxygenation. The observed isotope pattern is identical to that simulated for **4** (Figure 1D). The smaller peak at *m/z* = 796.59 is indicative of C(sp^2)–H bond oxygenation to generate complex $[LFe_3(HFArPz)_2(OFArPz)OFe][OTf]_2$ (**5**).[15] The peaks for **5** partially overlap with the peak at *m/z* = 799.10, associated with $[LFe_3(HFArPz)_3OFe(F)][OTf]_2$, which results from fluoride capture by starting material **1**, coupled with one electron oxidation.[16] The preference for C(sp^2)–F bond oxygenation is further supported by ^{1}H NMR spectroscopy by comparison of the reaction mixture to authentic samples of **4** and **5**. Visual inspection revealed that **4** is indeed the major species (Figure S8). In order to quantify the ratio between C(sp^2)–H and C(sp^2)–F bond oxygenation, a calibration curve was constructed by integrating the resonances at 31.8 ppm and 33.0 ppm, upon mixing **4** and **5** in known concentrations (Figure 1F and Figure S9; blue dots and dashed black trace). Integration of the corresponding peaks in the ^{1}H NMR spectrum of crude reaction mixture revealed a C(sp^2)–F to C(sp^2)–H ratio of approximately 8 to 1 (Figure 1F, green dots). A similar ratio (9 to 1) was determined based on mass spectrometry data (Figures S18–S20). Integration of the ^{1}H-NMR peaks in the presence of an internal standard (Figure S28 and S29), reveals that conversion to **4** and **5** occurs between 40–50%. An alternative determination of the yield and conversion that relied on acid mediated hydrolysis of the organic fragments was not successful. Nonetheless, the NMR and ESI-MS data unequivocally demonstrate that C(sp^2)–F bond oxygenation is the preferred reactivity pathway by almost an order of magnitude (Table 1). The preference for C(sp^2)–F bond oxygenation is notable, given that the preferred reactivity pathway for most terminal high-valent metal oxo complexes, including P450s, is C(sp^2)–H bond hydroxylation (*vide supra*).[6] Only three other studies have reported selective C(sp^2)–F oxygenation in the presence of other C(sp^2)–H bonds.[12]

To gain further insight into the selectivity of C(sp^2)–F bond oxygenation, modifications pertinent to the nature of the apical and core metal centers were performed taking advantage of our stepwise synthetic protocol (Scheme 1).[11b, 13] Metal-based effects on C(sp^2)–F vs C(sp^2)–H bond oxygenation for isostructural compounds have not been reported to our knowledge. Consequently, isostructural complexes $[LM_3(HFArPz)_3OMn][OTf]_2$ (**2;** M = Fe, **3**; M = Mn) were synthesized (Figures S4–S5).

Addition of ^{s}PhIO (2.0 equiv.) to a solution of complex **2** resulted in the oxygenation of both C(sp^2)–F and C(sp^2)–H bonds as judged by ESI-MS (Figure S21–S23) and ^{1}H NMR spectroscopy (Figures S12 and S13). Based on known ratios of authentic samples of $[LFe_3(HFArPz)_2(OArPz)OMn][OTf]_2$ (**6;** *m/z* = 787.59) and $[LFe_3(HFArPz)_2(OFArPz)OMn][OTf]_2$ (**7**; *m/z* = 796.09), the experimental ratio was determined at *ca.*1 to 1.3, favoring C(sp^2)–H bond oxygenated product **6** (Figure S23A). Using the same procedure, the calibration curve constructed by ^{1}H NMR spectroscopy revealed a nearly identical ratio of *ca.* 1 to 2 (Figure S23B). Similar results were obtained upon treating **3** with ^{s}PhIO (2.0 equiv.). Based on the ESI-MS data, the experimental ratio of $[LMn_3(HFArPz)_2(OArPz)OMn][OTf]_2$ (**8;** *m/z* = 787.59) to $[LMn_3(HFArPz)_2(OFArPz)OMn][OTf]_2$ (**9**; *m/z* = 796.09) reveals that C(sp^2)–H bond oxygenation is clearly favored (Figure S24). However, due the paramagnetic broadening by manganese, and difficulties in obtaining sufficiently pure authentic samples of complexes **8** and **9**, a definite C(sp^2)–F to C(sp^2)–H ratio could not be determined. Nevertheless, the oxygenation studies with **2** and **3** indicate that manganese is competent for C(sp^2)–F bond oxygenation. Notably, while Mn-oxo species have been employed for C–H bond halogenation reactions,[17] defluorination reaction involving Mn-oxo species have not been reported to the best of our knowledge. The observed reactivity with complexes **2** and **3** thus demonstrate the first examples of C(sp^2)–F bond oxygenation by a putative Mn-oxo species, albeit at a lower selectivity compared to iron (Table 1). While for complex **1** almost exclusive C(sp^2)–F bond oxygenation is observed,[16] the main reactivity pathway for complexes that contain manganese as apical metal center (**2** and **3**) is C(sp^2)–H bond oxygenation.[15]

The metal-based selectivity in intramolecular oxygenation with complexes **1**–**3** is intriguing, where the preference for C(sp^2)–F over C(sp^2)–H bond oxygenation with complex **1** is unusual. While many computational studies have investigated the effect of fluorine substituents on benzene C(sp^2)–H hydroxylation,[18] C(sp^2)–F bond hydroxylation in the presence of C–H bonds has been evaluated less, likely due to lack of experimental demonstrations until recently.[12] In the cases where C(sp^2)–F bond oxygenation is observed, a mechanism similar to that for benzene hydroxylation has been proposed.[11d, 12a, 19] For hexafluorobenzene, a rate limiting electrophilic attack of an Fe^{IV}-oxo on the π-system of the fluoroarene was proposed, which is followed by fluorine NIH shift. [19] Although rare, such fluorine NIH shifts have been observed. [12a, 20] However, independent syntheses of **5** and **7**, do not suggest such an NIH shift in the present system.[21] Related mechanisms for C(sp^2)–F activation have been proposed as well.[11d] In these mechanistic proposals, after the initial electrophilic attack by a metal-oxo, a fluoride anion is eliminated upon electron transfer to the arene ring.[11d] Such a pathway might be operating here as well, where the basal metal centers could participate in these redox processes by providing the required reducing equivalents. The selectivity of C(sp^2)–F vs C(sp^2)–H bond oxygenation, nonetheless, remain unclear. We speculate that the observed differences might be related to the extent of stabilization of the developing cationic/radical character on the arene ring *en-route* to the Meisenheimer σ-complex.[1f, 19] Fluorine might play a pivotal role in this stabilization, as it is known to stabilize organic radicals.[22]

Due to the multinuclear nature of the studied complexes and the accessibility of multiple oxidation states, a mechanism involving nucleophilic aromatic substitution of fluoride from a M(III)-oxide moiety – generated by electron transfer from the trimetallic core to an intermediate M(IV)-oxo species – cannot be ruled out. Such nucleophilic intermediates may be more accessible with the more reducing and electron rich clusters. In agreement with this hypothesis, the higher C(sp^2)–F bond oxygenation selectivity of **1** correlates with the most negative $M^{III}_2M^{II}_2/M^{III}_3M^{II}$ redox couple of compounds **1**–**3**, although the difference with **2** is small. Such correlation between the reduction potentials of **1**–**3** and the reactivity of the proposed metal-oxo species must be taken cautiously, however, as the structures and oxidation states of the precursors and reactivity intermediates are different.

In summary, we employed a series of Mn and Fe clusters to study the selectivity of oxygenation of aromatic C(sp^2)–F and C(sp^2)–H bonds. We demonstrate that Mn is competent for defluorination of a pendant fluoroarene via a putative Mn-oxo species. The selectivity of bond activation is distinct for the proposed Fe- and Mn-oxo moieties. While for iron, C(sp^2)–F bond oxygenation is observed almost exclusively, for manganese, C(sp^2)–H oxygenation is slightly preferred. These results may inform the development of selective transformation for bond breaking/forming reaction involving fluorine.

Supplementary Material

Refer to Web version on PubMed Central for supplementary material.

Acknowledgments

This research was supported by the NIH (R01-GM102687B). T.A. is grateful for a Dreyfus fellowship. K.M.C. is grateful for a Summer Undergraduate Research Fellowship. We thank Lawrence M. Henling for assistance with X-ray crystallography. We would also like to thank Mona Shahgholi for assistance with mass spectrometry.

References

1. (a) Ray K, Heims F, Schwalbe M, Nam W. Curr Opin Chem Biol. 2015; 25:159–171. [PubMed: 25703840] (b) Yano J, Yachandra V. Chem Rev. 2014; 114:4175–4205. [PubMed: 24684576] (c) Que L. Bull Jpn Soc Coord Chem. 2013; 62:30–37. [PubMed: 25678937] (d) Ortiz de Montellano PR. Chem Rev. 2010; 110:932–948. [PubMed: 19769330] (e) Rittle J, Green MT. Science. 2010; 330:933–937. [PubMed: 21071661] (f) Shaik S, Cohen S, Wang Y, Chen H, Kumar D, Thiel W. Chem Rev. 2010; 110:949–1017. [PubMed: 19813749] (g) Krebs C, Galonić Fujimori D, Walsh CT, Bollinger JM. Acc Chem Res. 2007; 40:484–492. [PubMed: 17542550] (h) Costas M, Mehn MP, Jensen MP, Que L. Chem Rev. 2004; 104:939–986. [PubMed: 14871146] (i) Meunier B, de Visser SP, Shaik S. Chem Rev. 2004; 104:3947–3980. [PubMed: 15352783]
2. (a) Ioannides, C., editor. Cytochromes P450; Role in the Metabolism and Toxicity of Drugs and Other Xenobiotics. Royal Society of Chemistry; 2008. (b) Guengerich FP. The AAPS Journal. 2006; 8:E101–E111. [PubMed: 16584116] (c) Anzenbacher P, Anzenbacherová E. Cell Mol Life Sci. 2001; 58:737–747. [PubMed: 11437235]
3. (a) Ullrich R, Hofrichter M. Cell Mol Life Sci. 2007; 64:271–293. [PubMed: 17221166] (b) Shimada T, Fujii-Kuriyama Y. Cancer Sci. 2004; 95:1–6. [PubMed: 14720319] (c) Rendic S. Drug Metab Rev. 2002; 34:83–448. [PubMed: 11996015]
4. Park BK, Kitteringham NR, O'Neill PM. Annu Rev Pharmacol Toxicol. 2001; 41:443–470. [PubMed: 11264465]
5. (a) Wang J, Sánchez-Roselló M, Aceña JL, del Pozo C, Sorochinsky AE, Fustero S, Soloshonok VA, Liu H. Chem Rev. 2014; 114:2432–2506. [PubMed: 24299176] (b) Hagmann WK. J Med Chem.

2008; 51:4359–4369. [PubMed: 18570365] (c) Böhm HJ, Banner D, Bendels S, Kansy M, Kuhn B, Müller K, Obst-Sander U, Stahl M. Chem Bio Chem. 2004; 5:637–643.

6. (a) Dennig A, Lülsdorf N, Liu H, Schwaneberg U. Angew Chem Int Ed. 2013; 52:8459–8462.(b) Rietjens IMCM, den Besten C, Hanzlik RP, van Bladeren PJ. Chem Res Toxicol. 1997; 10:629–635. [PubMed: 9208168] (c) Rietjens IMCM, Soffers AEMF, Veeger C, Vervoort J. Biochemistry. 1993; 32:4801–4812. [PubMed: 8490024]
7. Rietjens IMCM, Vervoort J. Chem Res Toxicol. 1992; 5:10–19. [PubMed: 1581524]
8. (a) Cnubben NHP, Vervoort J, Boersma MG, Rietjens IMCM. Biochem Pharmacol. 1995; 49:1235–1248. [PubMed: 7763304] (b) Cnubben NHP, Vervoort J, Veeger C, Rietjens IMCM. Chem-Biol Interact. 1992; 85:151–172. [PubMed: 1493607] (c) Rietjens IMCM, Tyrakowska B, Veeger C, Vervoort J. Eur J Biochem. 1990; 194:945–954. [PubMed: 2269311]
9. (a) Ohe T, Mashino T, Hirobe M. Drug Metab Dispos. 1997; 25:116–122. [PubMed: 9010638] (b) den Besten C, van Bladeren PJ, Duizer E, Vervoort J, Rietjens IMCM. Chem Res Toxicol. 1993; 6:674–680. [PubMed: 8292746] (c) Rietjens IMCM, Vervoort J. Chem-Biol Interact. 1991; 77:263–281. [PubMed: 2009574]
10. (a) Sahu S, Widger LR, Quesne MG, de Visser SP, Matsumura H, Moënne-Loccoz P, Siegler MA, Goldberg DP. J Am Chem Soc. 2013; 135:10590–10593. [PubMed: 23834409] (b) Thibon A, Jollet V, Ribal C, Sénéchal-David K, Billon L, Sorokin AB, Banse F. Chem Eur J. 2012; 18:2715–2724. [PubMed: 22290835] (c) Bigi JP, Harman WH, Lassalle-Kaiser B, Robles DM, Stich TA, Yano J, Britt RD, Chang CJ. J Am Chem Soc. 2012; 134:1536–1542. [PubMed: 22214221] (d) Makhlynets OV, Rybak-Akimova EV. Chem Eur J. 2010; 16:13995–14006. [PubMed: 21117047] (e) Makhlynets OV, Das P, Taktak S, Flook M, Mas-Ballesté R, Rybak-Akimova EV, Que L. Chem Eur J. 2009; 15:13171–13180. [PubMed: 19876966] (f) Harman WH, Chang CJ. J Am Chem Soc. 2007; 129:15128–15129. [PubMed: 18004860] (g) de Visser SP, Oh K, Han AR, Nam W. Inorg Chem. 2007; 46:4632–4641. [PubMed: 17444641] (h) Nielsen A, Larsen FB, Bond AD, McKenzie CJ. Angew Chem Int Ed. 2006; 45:1602–1606.(i) Oh NY, Seo MS, Lim MH, Consugar MB, Park MJ, Rohde JU, Han J, Kim KM, Kim J, Que JL, Nam W. Chem Commun. 2005:5644–5646.(j) Mehn MP, Fujisawa K, Hegg EL, Que L. J Am Chem Soc. 2003; 125:7828–7842. [PubMed: 12823001] (k) Jensen MP, Mehn MP, Que L. Angew Chem Int Ed. 2003; 42:4357–4360.(l) Mekmouche Y, Ménage S, Toia-Duboc C, Fontecave M, Galey JB, Lebrun C, Pécaut J. Angew Chem Int Ed. 2001; 40:949–952.(m) Hegg EL, Ho RYN, Que L. J Am Chem Soc. 1999; 121:1972–1973.
11. (a) Garcia-Bosch I, Cowley RE, Díaz DE, Peterson RL, Solomon EI, Karlin KD. J Am Chem Soc. 2017; 139:3186–3195. [PubMed: 28195739] (b) Carsch KM, de Ruiter G, Agapie T. Manuscript in preparation. 2017c de Ruiter G, Thompson NB, Takase MK, Agapie T. J Am Chem Soc. 2016; 138:1486–1489. [PubMed: 26760217] d Sahu S, Zhang B, Pollock CJ, Dürr M, Davies CG, Confer AM, Ivanović-Burmazović I, Siegler MA, Jameson GNL, Krebs C, Goldberg DP. J Am Chem Soc. 2016; 138:12791–12802. [PubMed: 27656776] (e) Sahu S, Quesne MG, Davies CG, Dürr M, Ivanović-Burmazović I, Siegler MA, Jameson GNL, de Visser SP, Goldberg DP. J Am Chem Soc. 2014; 136:13542–13545. [PubMed: 25246108]
12. (a) Colomban C, Kudrik EV, Afanasiev P, Sorokin AB. J Am Chem Soc. 2014; 136:11321–11330. [PubMed: 25031156] (b) Serrano-Plana J, Garcia-Bosch I, Miyake R, Costas M, Company A. Angew Chem Int Ed. 2014; 53:9608–9612.(c) Ohe T, Mashino T, Hirobe M. Tetrahedron Lett. 1995; 36:7681–7684.
13. de Ruiter G, Carsch KM, Gul S, Chatterjee R, Thompson NB, Takase MK, Yano J, Agapie T. Angew Chem Int Ed. 2017; 56:4772–4776.
14. (a) de Ruiter G, Thompson NB, Lionetti D, Agapie T. J Am Chem Soc. 2015; 137:14094–14106. [PubMed: 26390375] (b) Herbert DE, Lionetti D, Rittle J, Agapie T. J Am Chem Soc. 2013; 135:19075–19078. [PubMed: 24304416]
15. The formation of $[LM_3(HFArPz)_2(OFArPz)OM']$[OTf]$_2$ (M = M′ = Mn or Fe), proceeds with the formal loss of a H-atom. Similar reactivity has been observed in the intramolecular C-H bond oxygenation with other metal complexes, where high-valent metal-oxos are invoked. See: references 13, 11c, 10c, and 10f.
16. The formation of $[LM_3(HFArPz)_2(OArPz)OM']$[OTf]$_2$ (M = M′ = Mn or Fe), proceeds with the formal loss of a fluoride anion. Since the oxygenation reaction is rapid, only small amounts of

$[LM_3(HFArPz)_3OM'(F)][OTf]$ are formed and, therefore, these species cannot serve as the reductant to balance the reaction as previously reported (for more details see reference 11c). Similar to C-H bond oxygenation (see ref 15), an unkown reductant is responsible for the formation of $[LM_3(HFArPz)_2(OArPz)OM'][OTf]_2$ (M = M′ = Mn or Fe).

17. Liu W, Groves JT. Acc Chem Res. 2015; 48:1727–1735. [PubMed: 26042637]
18. (a) Shaik S, Milko P, Schyman P, Usharani D, Chen H. J Chem Theory Comput. 2011; 7:327–339. [PubMed: 26596155] (b) Bathelt CM, Ridder L, Mulholland AJ, Harvey JN. Org Biomol Chem. 2004; 2:2998–3005. [PubMed: 15480465] (c) Bathelt CM, Ridder L, Mulholland AJ, Harvey JN. J Am Chem Soc. 2003; 125:15004–15005. [PubMed: 14653732] (d) Zakharieva O, Grodzicki M, Trautwein AX, Veeger C, Rietjens IMCM. J Biol Inorg Chem. 1996; 1:192–204.
19. Hackett JC, Sanan TT, Hadad CM. Biochemistry. 2007; 46:5924–5940. [PubMed: 17455915]
20. Koerts J, Soffers AEMF, Vervoort J, De Jager A, Rietjens IMCM. Chem Res Toxicol. 1998; 11:503–512. [PubMed: 9585481]
21. By ESI-MS, products generated from a fluorine NIH shift would be indistinguishable from a pathway involving $C(sp^2)$–H bond oxygenation. As stated, ^1H NMR spectroscopy rules out such a mechanism, unless the ^1H NMR spectra these species are identical to those of 5 and 7, which we regard as highly unlikely.
22. (a) Bernardi F, Cherry W, Shaik S, Epiotis ND. J Am Chem Soc. 1978; 100:1352–1356.(b) Zipse H. Top Curr Chem. 2006; 263:163–189.(c) Coote ML, Lin CY, Beckwith ALJ, Zavitsas AA. Phys Chem Chem Phys. 2010; 12:9597–9610. [PubMed: 20556274]

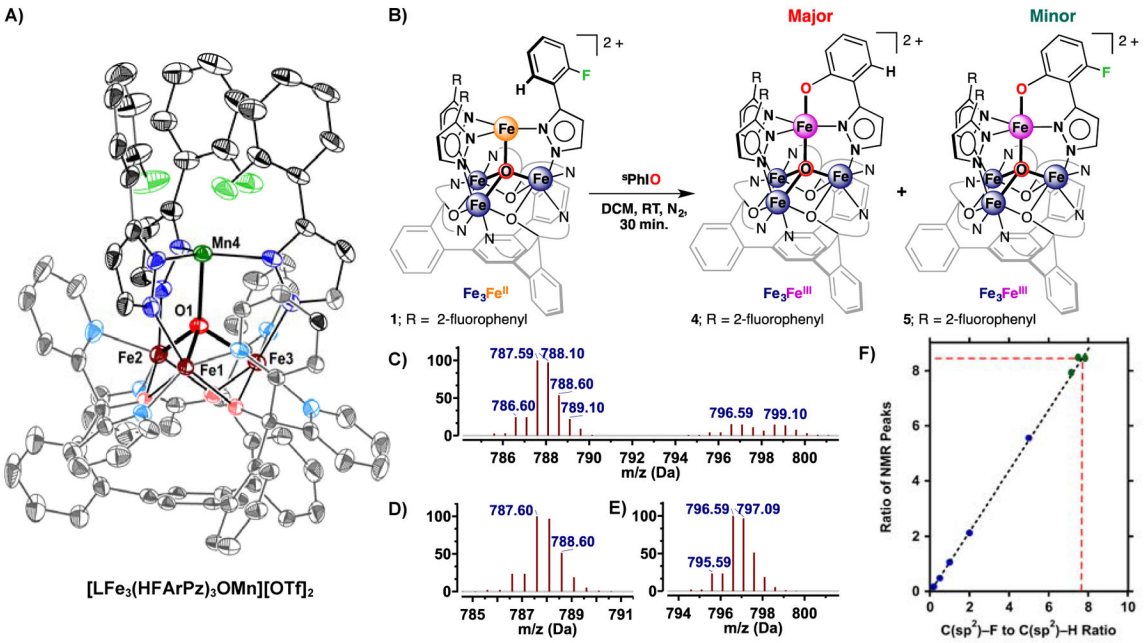

Figure 1.

(A) Crystal structure of $[LFe_3(HFArPz)_3OMn][OTf]_2$ (**2**). Thermal ellipsoids are shown at the 50% probability level. Hydrogen atoms, outer sphere counter ions, and co-crystallized solvent molecules are not shown for clarity. See Table S1 for a summary of selected bond-distances and angles. (B) Formation of complexes **4** and **5** by treating complex **1** with ^{s}PhIO (2 equiv.) for 30 minutes in CH_2Cl_2. (C) Electrospray ionization mass spectrum (ESI-MS) of an aliquot of the crude reaction mixture after treating **1** with ^{s}PhIO (2 equiv.) for 30 minutes in CH_2Cl_2. (D–E) Simulated mass spectrum and isotope distribution pattern for **4** $[C_{84}H_{57}F_2Fe_4N_{12}O_5]^{2+}$ and **5** $[C_{84}H_{56}F_3Fe_4N_{12}O_5]^{2+}$. (F) Experimentally determined $C(sp^2)$–F to $C(sp^2)$–H ratio (green dots), by integrating the ^{1}H NMR resonances at 31.8 ppm and 33.0 ppm belonging to complexes **4** and **5** respectively. The blue dots and dashed black trace ($R^2 = 0.99$) represent the calibration curve obtained by recording the ratio of the ^{1}H NMR signals at 31.8 ppm and 33.0 ppm upon mixing known concentrations of complexes **4** and **5**.

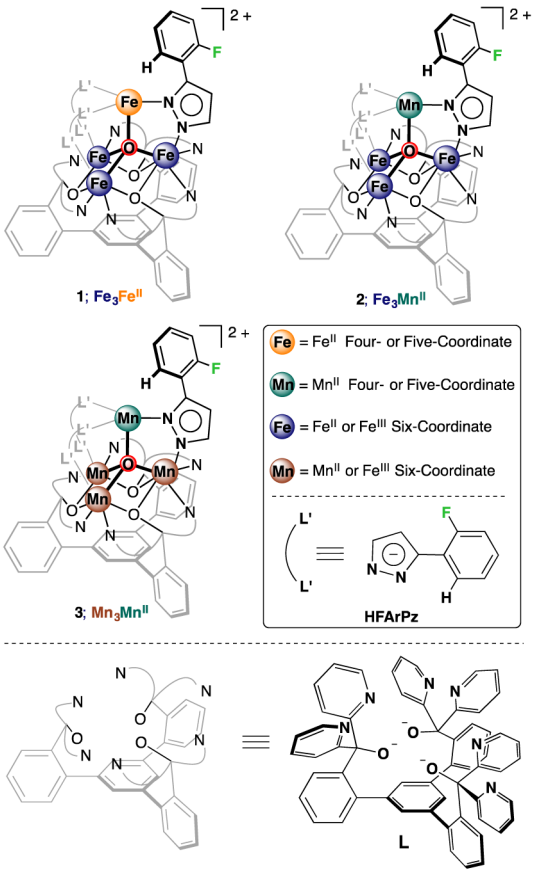

Scheme 1.

General molecular structure of complexes **1**–**3**, supported by pyrazolates and a 1,3,5-triarylbenzene-based ligand (L). The inset shows the coloring scheme for the apical and core metal centers.

Table 1

Oxidation potential and reactivity pathways for complexes **1**–**3**.

#	$E_{½}$ (Fc/Fc$^+$) $M^{III}_2M^{II}_2/M^{III}_3M^{II}$	C(sp^2)–F vs. C(sp^2)–H Oxygenation	
		Preferred Pathway	Ratio[a]
1	− 0.08 V	C(sp^2)–**F**	> 8:1
2	− 0.02 V	C(sp^2)–**H**	1:1 – 1:2
3	+ 0.26 V	C(sp^2)–**H**	ND

[a]Determined my mass spectrometry and ^{1}H NMR spectroscopy; see Figure 1F, Figure 2, and the supporting information for experimental details.